



7-21-2017

Inverse-Kinematics Proton Scattering on 43P

Lisa M. Skiles

Ursinus College, liskiles@ursinus.edu

Follow this and additional works at: https://digitalcommons.ursinus.edu/physics_astro_sum



Part of the [Physics Commons](#)

Click here to let us know how access to this document benefits you.

Recommended Citation

Skiles, Lisa M., "Inverse-Kinematics Proton Scattering on 43P" (2017). *Physics and Astronomy Summer Fellows*. 16.
https://digitalcommons.ursinus.edu/physics_astro_sum/16

This Paper is brought to you for free and open access by the Student Research at Digital Commons @ Ursinus College. It has been accepted for inclusion in Physics and Astronomy Summer Fellows by an authorized administrator of Digital Commons @ Ursinus College. For more information, please contact aprock@ursinus.edu.

Inverse-Kinematics Proton Scattering on ^{43}P

L. M. Skiles

(Dated: July 20, 2017)

Abstract

Following an experiment at the National Superconducting Cyclotron Laboratory at Michigan State University in October 2016, we study the excited states of the neutron-rich $N=28$ isotope ^{43}P via inverse-kinematics proton scattering with the NSCL/Ursinus College liquid hydrogen target and the GRETINA γ -ray tracking array. We discuss preliminary analysis and results, including measured cross sections for populating excited states of ^{43}P .

EXPERIMENT

The experiment took place at the National Superconducting Cyclotron Laboratory at Michigan State University (NSCL). A primary beam of 140 MeV/u ^{48}Ca was incident on a 1222 mg/cm² ^9Be primary target. The resulting fragments formed a secondary beam, which was separated by the A1900 fragment separator [1]. The secondary beam then passed through the Ursinus College Liquid Hydrogen Target located at the pivot point of the S800 magnetic spectrograph [2]. Beam particles were identified upstream of the target using the time of flight from the A1900 extended focal plane scintillator and the S800 object scintillator to the E1 scintillator, shown in Figure 1. The beam-like reaction products were identified using energy loss in the S800 ion chamber and the time of flight from the S800 object scintillator to a scintillator in the focal plane of the S800, as shown in Figure 2. The beam was composed of 45.1% ^{44}S , 45.2% ^{46}Cl , and 8.4% ^{43}P , the latter of which is the focus of this work.

The GRETINA γ -ray tracking array [3] was focused on the liquid hydrogen target at the pivot point of the S800. All coincidence events between GRETINA and the S800 were collected. In addition, all events in the S800 were collected in order to determine the total number of particles passing through the target during the experiment. In the case of ^{43}P , the total was $1.39 \cdot 10^8$, or 2420 particles per second.

ANALYSIS AND RESULTS

GEANT4 [4] simulations were used to simulate the beam passing through the target and the emission and detection of γ -rays. In order to accurately simulate γ -rays emitted in flight by beam particles slowing down in the target, simulated relative kinetic energy spectra were fitted to measured spectra. This also allows for determination of the optimal average speed for Doppler correction of γ -ray spectra.

The liquid hydrogen target consisted of a 30 mm thick aluminum cell, with 125 μm Kapton entrance and exit windows. Due to the pressure difference between the cell and the vacuum inside the beam line, the windows deformed, adding to the overall thickness of the target. To determine the window bulge thickness, simulations varying bulge thickness were fit to the measured relative kinetic energy spectrum. The relative kinetic energy of the beam

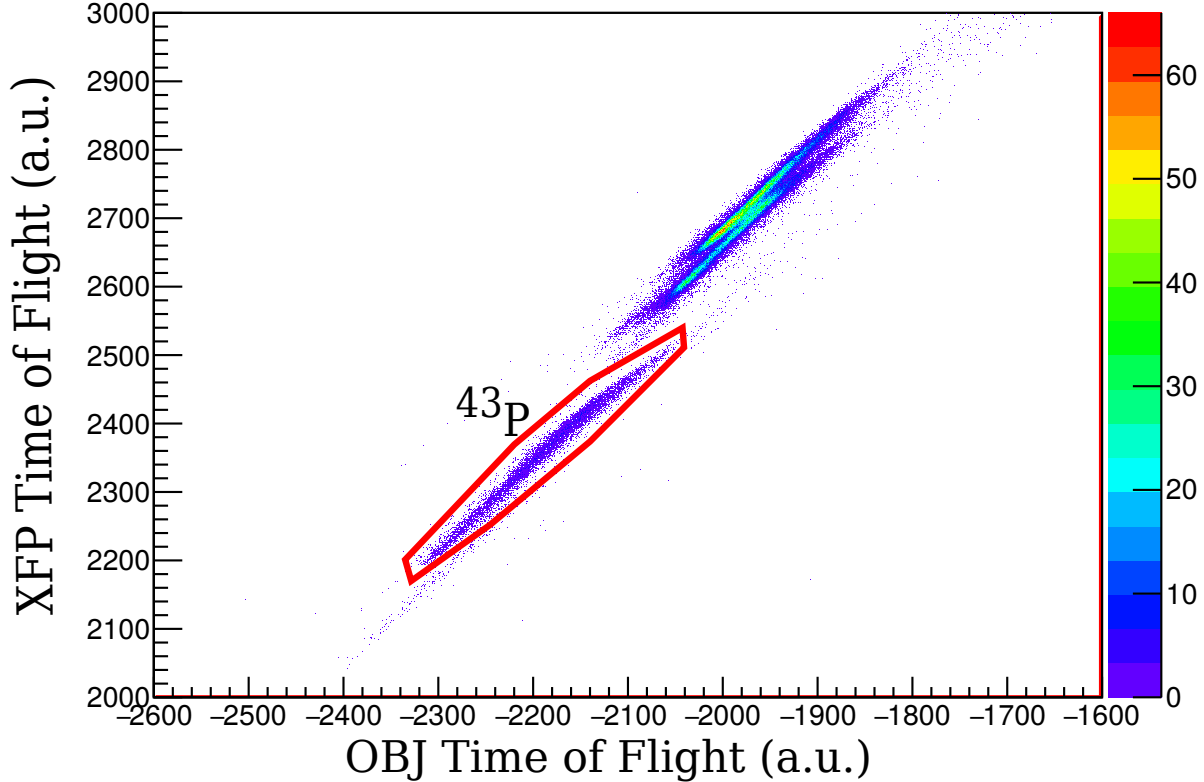


FIG. 1. Incoming particle identification spectrum generated by the time of flight from the S800 object scintillator (OBJ) on the horizontal axis and that from the A1900 extended focal plane scintillator (XFP) on the vertical axis. The E1 scintillator in the S800 focal plane stopped both time measurements. The red contour is the cut for ^{43}P .

is given by

$$\frac{(KE - KE_0)}{KE_0} \quad (1)$$

where KE is the measured kinetic energy of the beam and KE_0 is the central kinetic energy of the S800. In the case of incoming ^{43}P beam, the average relative kinetic energy is 0.0025 and $KE_0 = 78.58$ MeV/u, meaning the average energy of the beam is $KE = 78.78$ MeV/u. The momentum spread of the incoming beam was $\Delta P/P = 2\%$. Figure 3 shows the experimental relative kinetic energy spectrum of the outgoing ^{43}P particles in black, compared with a simulated spectrum in blue assuming a 1.2 mm bulge thickness of the target windows, shown in Figure 4.

Assuming known γ -ray energies [5], the simulated spectrum can then be used to determine

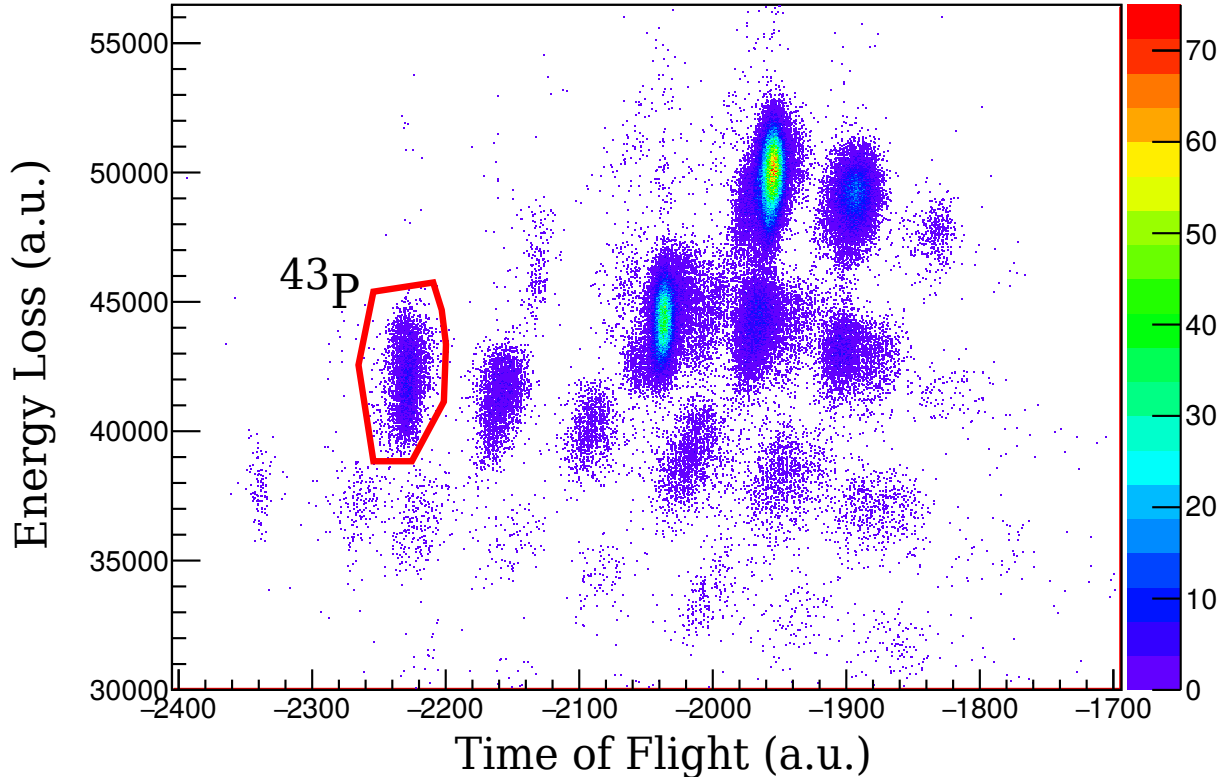


FIG. 2. Outgoing particle identification spectrum consisting of the energy loss in the S800 ion chamber versus the time of flight from the S800 object scintillator to the E1 scintillator in the focal plane of the S800. The red contour is the ^{43}P cut.

the offset of the target along the beam axis. Simulations that varied values for the target offset were fit to measured γ -ray spectra and minimized to find the optimal offset value for all γ -ray energies, as shown in Figure 5. For the beam containing ^{43}P , the target offset was determined to be 7.2 mm.

Once the target offset was determined using known γ -ray energies[5], simulations were then used to find best-fit energies by varying γ -ray energies and minimizing the figure of merit from the fit. Known and measured γ -ray energies are compared in Table I. In the case of the first excited state, the half life of the state was also considered. In addition to varying energy levels, half life values were also varied in simulations to best fit the peak. The half life of the first excited state was determined to be 125.6 ps. Figure 6 shows the measured γ -ray energy spectrum in black, and the the Doppler corrected simulated γ -ray spectrum in blue, using the optimized energy values.

After γ -ray energies were optimized, the excited states of ^{43}P were placed into a proposed

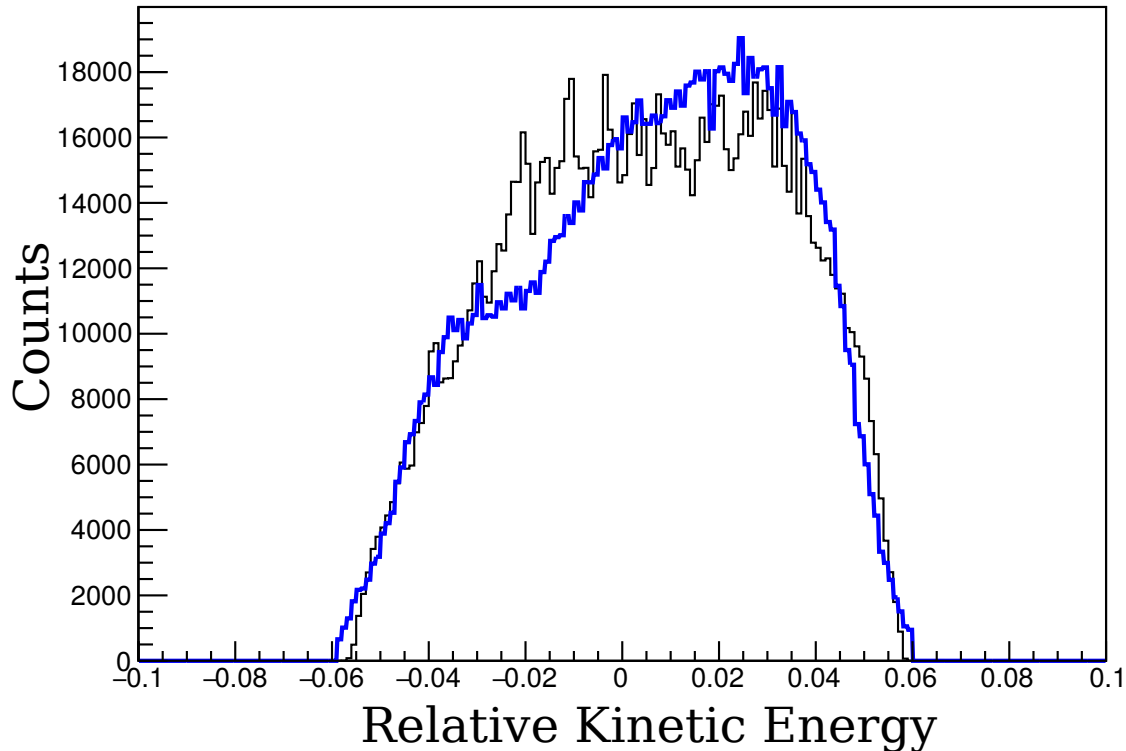


FIG. 3. Relative kinetic energy spectrum of ^{43}P with a simulated target bulge thickness of 1.2 mm. The blue curve is the simulated spectrum, while the black curve shows the experimental spectrum.

energy level diagram. Shown in Figure 7, the energy level diagram includes γ -ray energies and intensities for each excited state, corresponding to values given in Figure 6. Measured relative intensities and branching ratios are included in Table I.

This work was supported by the National Science Foundation under Grant Nos. PHY-1617250. GRETINA was funded by the US DOE - Office of Science. Operation of the array at NSCL is supported by NSF under Cooperative Agreement No. PHY-1102511(NSCL) and DOE under Grant No. DE-AC02-05CH11231 (LBNL). We also thank T. J. Carroll for the use of the Ursinus College Parallel Computing Cluster, which is supported by NSF Grant No. PHY-1607335.

[1] D. J. Morrissey, B. M. Sherrill, M. Steiner, A. Stolz, and I. Wiedenhoefer, Nuclear Instruments and Methods in Physics Research Section B: Beam Interactions with Materials and Atoms **204**,

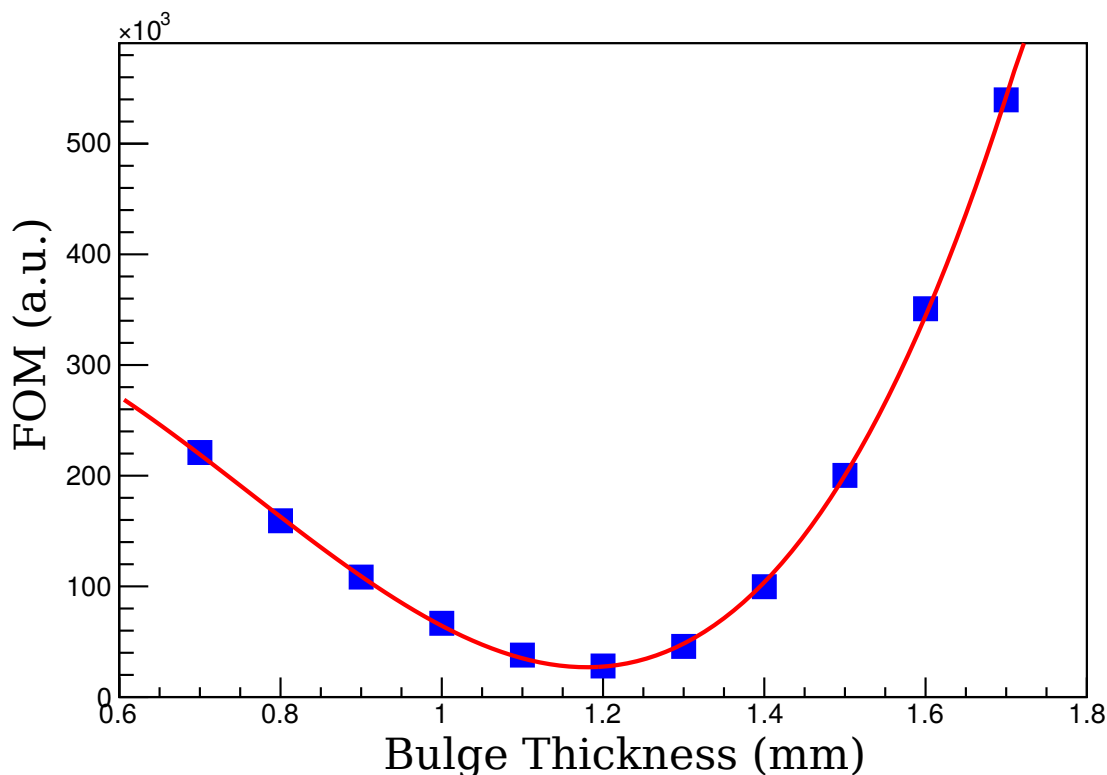


FIG. 4. Simulated values for the target window bulge thickness. The red curve represents a polynomial fit used to minimize the function and find the bulge thickness of the target.

90 (2003).

- [2] D. Bazin, J. A. Caggiano, B. M. Sherrill, J. Yurkon, and A. Zeller, Nuclear Instruments and Methods in Physics Research Section B: Beam Interactions with Materials and Atoms **204**, 629 (2003).
- [3] I.-Y. Lee, J. Phys.: Conf. Ser. **420**, 012156 (2013).
- [4] S. Agostinelli, J. Allison, K. Amako, J. Apostolakis, H. Araujo, P. Arce, M. Asai, D. Axen, S. Banerjee, G. Barrand, F. Behner, L. Bellagamba, J. Boudreau, L. Broglia, A. Brunengo, H. Burkhardt, S. Chauvie, J. Chuma, R. Chytracsek, G. Cooperman, G. Cosmo, P. Degt-yarenko, A. Dell’Acqua, G. Depaola, D. Dietrich, R. Enami, A. Feliciello, C. Ferguson, H. Fesefeldt, G. Folger, F. Foppiano, A. Forti, S. Garelli, S. Giani, R. Giannitrapani, D. Gibin, J. J. Gmez Cadenas, I. Gonzalez, G. Gracia Abril, G. Greeniaus, W. Greiner, V. Grichine, A. Grossheim, S. Guatelli, P. Gumplinger, R. Hamatsu, K. Hashimoto, H. Hasui, A. Heikkinen, A. Howard, V. Ivanchenko, A. Johnson, F. W. Jones, J. Kallenbach, N. Kanaya, M. Kawa-

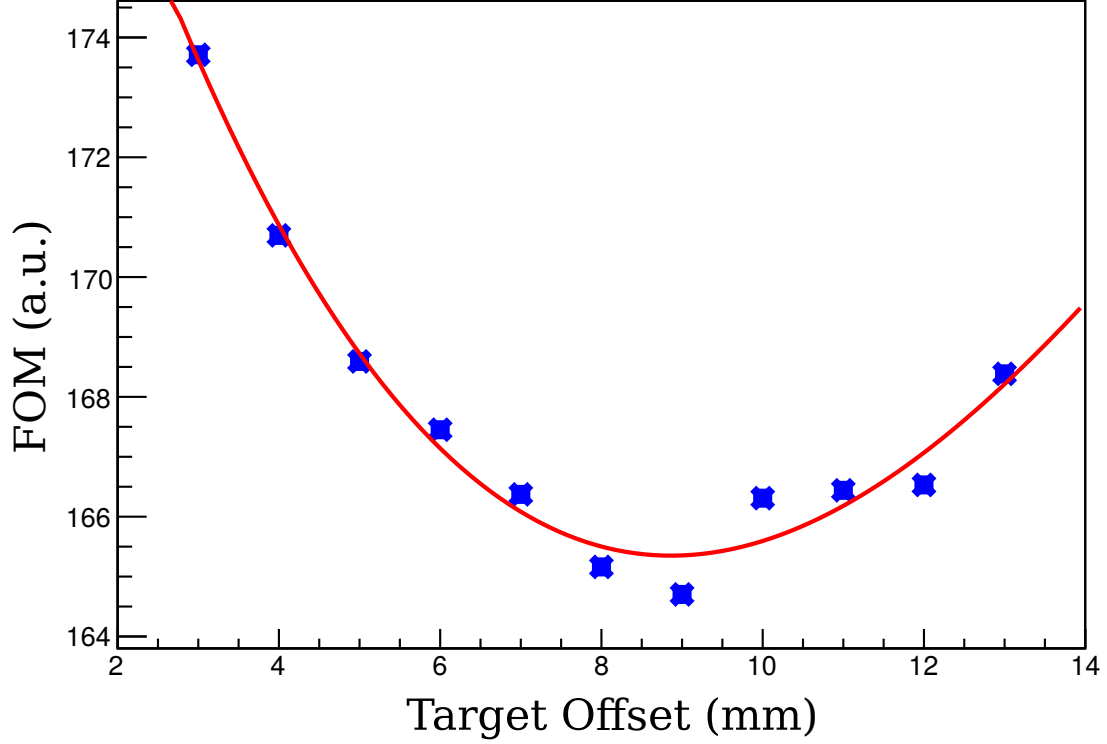


FIG. 5. Simulated z offset values for the liquid hydrogen target position. The red curve represents a polynomial fit used to minimize the function and find the optimal target position.

TABLE I. Level energies, spins and parities, and γ -ray energies from Ref. [5], γ -ray energies, intensities relative to that of the $2_1^+ \rightarrow 0_{g.s.}^+$ transitions, branching ratios (BR), and cross sections from the present work.

	Refs. [5]				Present work		
	E_{level} [keV]	J^π [\hbar]	E_γ [keV]	BR [%]	E_γ [keV]	I_γ [%]	BR [%]
^{43}P	0	$1/2^+$		24(4)	0		0
	184	$3/2^+$	184(1)	33(2)	189()	100	0
	845	$(5/2^+)$	661(4)	4(1)	661(4)	11	36
			845(4)		844(8)	47	64
	1009	$(5/2^+)$	825(5)	8(2)	820(2)	20	0
	1095	$(5/2^+)$	911(6)	20(1)	913(4)	30	0
	2035	$(5/2^+)$	1018(6)	7(2)	1018(6)	14	77
			1851(11)		1851(11)	4	23

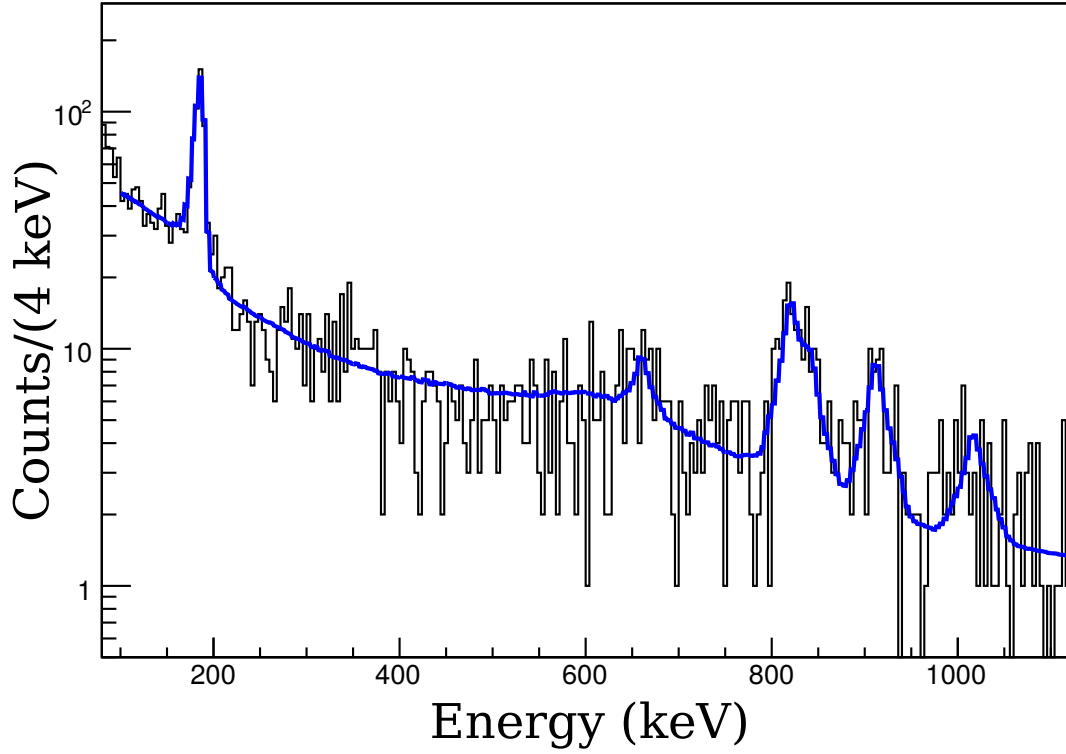


FIG. 6. Doppler-corrected γ -ray spectrum measured in coincidence with incoming and outgoing ^{43}P particles. The black curve is the measured spectrum, and the blue curve is the fit of the GEANT4 simulations described in the text.

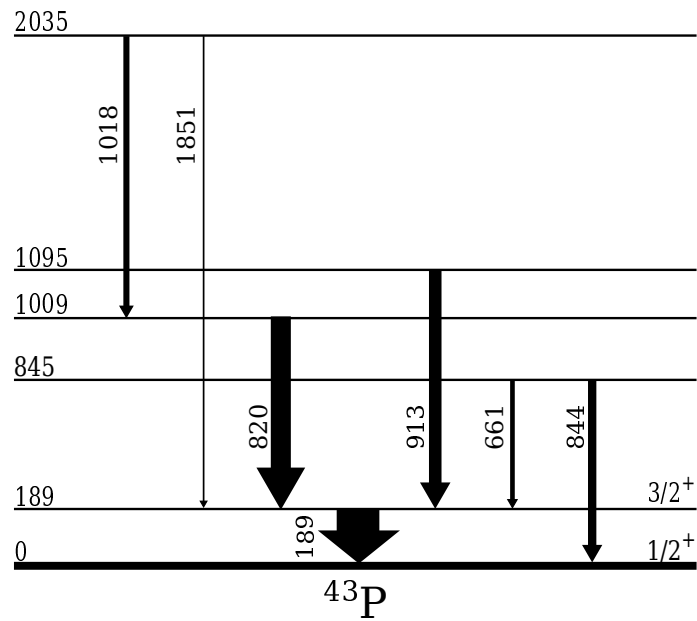


FIG. 7. Proposed level scheme for excited states of ^{43}P populated in the present work.

bata, Y. Kawabata, M. Kawaguti, S. Kelner, P. Kent, A. Kimura, T. Kodama, R. Kokoulin, M. Kossov, H. Kurashige, E. Lamanna, T. Lampn, V. Lara, V. Lefebure, F. Lei, M. Liendl, W. Lockman, F. Longo, S. Magni, M. Maire, E. Medernach, K. Minamimoto, P. Mora de Freitas, Y. Morita, K. Murakami, M. Nagamatu, R. Nartallo, P. Nieminen, T. Nishimura, K. Ohtsubo, M. Okamura, S. O’Neale, Y. Oohata, K. Paech, J. Perl, A. Pfeiffer, M. G. Pia, F. Ranjard, A. Rybin, S. Sadilov, E. Di Salvo, G. Santin, T. Sasaki, N. Savvas, Y. Sawada, S. Scherer, S. Sei, V. Sirotenko, D. Smith, N. Starkov, H. Stoecker, J. Sulkimo, M. Takahata, S. Tanaka, E. Tcherniaev, E. Safai Tehrani, M. Tropeano, P. Truscott, H. Uno, L. Urban, P. Urban, M. Verderi, A. Walkden, W. Wander, H. Weber, J. P. Wellisch, T. Wenaus, D. C. Williams, D. Wright, T. Yamada, H. Yoshida, and D. Zschesche, Nuclear Instruments and Methods in Physics Research Section A: Accelerators, Spectrometers, Detectors and Associated Equipment **506**, 250 (2003).

- [5] L. A. Riley, P. Adrich, T. R. Baugher, D. Bazin, B. A. Brown, J. M. Cook, P. D. Cottle, C. A. Diget, A. Gade, D. A. Garland, T. Glasmacher, K. E. Hosier, K. W. Kemper, T. Otsuka, W. D. M. Rae, A. Ratkiewicz, K. P. Siwek, J. A. Tostevin, Y. Utsuno, and D. Weisshaar, Phys. Rev. C **78**, 011303 (2008), copyright (C) 2010 The American Physical Society; Please report any problems to prola@aps.org.